



PERGAMON

International Journal of Heat and Mass Transfer 42 (1999) 3873–3885

International Journal of
**HEAT and MASS
TRANSFER**

www.elsevier.com/locate/ijhmt

Heat transfer by fully developed flow and viscous heating in a vertical channel with prescribed wall heat fluxes

Antonio Barletta*

*Dipartimento di Ingegneria Energetica, Nucleare e del Controllo Ambientale (DIENCA), Università di Bologna,
Viale Risorgimento 2, I-40136 Bologna, Italy*

Received 11 November 1998

Abstract

An analysis of combined forced and free convection in a vertical parallel-plate channel with prescribed wall heat fluxes is performed by considering a fully developed flow and by taking into account the effect of viscous dissipation. It is shown that the condition of fully developed flow cannot be accomplished if a streamwise change of the wall heat fluxes occurs. An analytical solution of the momentum balance and energy balance equations is found by a perturbation method. In particular, the forced convection flow with viscous heating is treated as the base heat transfer process. Then, the effect of buoyancy is accounted for by expressing the fluid velocity and temperature as power series with respect to the ratio between the Grashof number and the Reynolds number. © 1999 Elsevier Science Ltd. All rights reserved.

Keywords: Mixed convection; Viscous dissipation; Perturbation methods

1. Introduction

In recent literature, most of the interest devoted to mixed convection in vertical ducts is due to the applications which range from the field of electronic devices to that of solar energy collectors. Several papers on this subject refer to parallel plate channels and deal either with the fully developed region or with the developing flow region [1–12]. The mathematical models described in these papers refer to three kinds of thermal boundary conditions: (a) prescribed uniform temperatures on both walls, which can be either equal or different; (b) prescribed uniform temperature on one of the walls and prescribed uniform heat flux on the

other wall; and (c) prescribed uniform heat fluxes on both walls.

For laminar flow, in the fully developed region, i.e. in the region so far from the channel entrance that the fluid velocity does not undergo appreciable changes in the streamwise direction, the boundary conditions (a) and (b) can be considered as special cases of the more general boundary condition (c). More precisely, if viscous dissipation is negligible, the boundary conditions (a) and (b) correspond, on both channel walls, to uniform heat fluxes such that their absolute values are equal but the signs are opposite. As a consequence, if boundary conditions (a) and (b) are adopted, no heat transfer occurs in the streamwise direction, while boundary condition (c) implies, in general, a streamwise change of the fluid temperature.

Yao [1] obtains an analytical solution of the developing flow heat transfer in a vertical channel with symmetric and uniform wall temperatures or with

* Tel.: +39-51-6443295; fax: +39-51-6443296.

E-mail address: antonio.barletta@mail.ing.unibo.it (A. Barletta)

Nomenclature

a, b	dimensionless constants employed in Eq. (47)
Br	$= \mu U_0^2 / (4Lq_-)$, Brinkman number
c_p	specific heat at constant pressure [J/(kg K)]
f_-, f_+	Fanning friction factors defined by Eq. (23)
g	gravitational acceleration [m/s ²]
Gr	$= 64g\beta\Delta TL^3/\nu^2$, Grashof number
j	non-negative integer
k	thermal conductivity [W/(m K)]
L	channel half-width [m]
n	non-negative integer
Nu_-, Nu_+	Nusselt numbers defined by Eq. (25)
p	pressure [Pa]
P	$= p + \rho_0 g X$, difference between the pressure and the hydrostatic pressure [Pa]
q_-, q_+	prescribed heat fluxes at $Y = -L$ and at $Y = L$, respectively [W/m ²]
r_c	radius of convergence of the perturbation series
R	$= q_+ / q_-$, ratio between the wall heat fluxes
Re	$= 4LU_0/\nu$, Reynolds number
T	temperature [K]
T_0	mean temperature defined by Eq. (2) [K]
u	$= U/U_0$, dimensionless velocity component in the X -direction [m/s]
$u_n(y)$	dimensionless functions defined by Eq. (26)
U	velocity component in the X -direction [m/s]
\mathbf{U}	velocity [m/s]
U_0	mean velocity defined by Eq. (11) [m/s]
V	velocity component in the Y -direction [m/s]
X	streamwise coordinate [m]
Y	transverse coordinate [m]
y	$= Y/L$, dimensionless transverse coordinate
y', y''	dummy integration variables

Greek symbols

β	thermal expansion coefficient [K ⁻¹]
ΔT	$= \mu U_0^2 / k$, reference temperature difference [K]
η	dimensionless parameter defined by Eq. (15)
η_n	dimensionless parameters defined by Eq. (29)
θ	$= (T - T_0) / \Delta T$, dimensionless temperature
$\theta_n(y)$	dimensionless functions defined by Eq. (27)
λ	$= -[L^2 / (\mu U_0)] dP/dX$, dimensionless pressure-drop parameter
λ_n	dimensionless parameters defined by Eq. (28)
μ	dynamic viscosity [Pa s]
ν	$= \mu / \rho_0$, kinematic viscosity [m ² /s]
ρ	mass density [kg/m ³]
ρ_0	mass density evaluated at $T = T_0$ [kg/m ³]
χ	dimensionless parameter defined by Eq. (56)

Superscript

$-$	modified dimensionless quantities defined by Eq. (48)
-----	---

symmetric and uniform wall heat fluxes. Aung and Worku [2,4] analyze the developing flow region for asymmetric wall temperatures or asymmetric wall heat

fluxes by employing a finite-difference method. Aung and Worku [3] perform an investigation of the fully developed flow in the case of asymmetric and uniform

wall temperatures and point out the conditions for the occurrence of flow reversal. Lavine [5,8] is concerned with fully developed combined convection in inclined parallel-plate channels and regards vertical channels as a special case. Either the evaluation of laminar velocity and temperature profiles [5] and the analysis of the stability of the laminar solution [8] are studied. Cheng et al. [6] and Hamadah and Wirtz [7] analyze the fully developed region and the flow reversal for the boundary conditions (a), (b) and (c). Chen and Chung [9,10] investigate the linear stability of the fully developed laminar solutions, either in the case of symmetric and uniform wall heat fluxes [9] or in the case of asymmetric and uniform wall temperatures [10]. Indeed, the results described in Refs. [1–10] are based on the assumption that the effect of viscous dissipation can be neglected.

Recently, Barletta [11] and Zanchini [12] have presented analyses on the fully developed combined convection in a vertical channel by taking into account the effect of viscous dissipation. Both the case of prescribed wall temperatures [11] and the case of boundary conditions of the third kind [12] are treated. In these papers, the evaluation of the velocity and temperature profiles is performed by means of a perturbation method. More precisely, for any fixed value of the ratio between the Grashof number and the Reynolds number, the solution of the momentum and energy balance equations is expressed as a power series with respect to a dimensionless parameter proportional to the Brinkman number. As is well known [13], the Brinkman number accounts for the relevance of viscous heating.

The aim of the present paper is to study the fully developed combined forced and free convection in a vertical channel by taking into account the effect of viscous dissipation in the case of prescribed wall heat fluxes. As pointed out above, in this case, the temperature field depends on the streamwise coordinate even in the fully developed region. In the following, it will be pointed out that no parallel flow solution can exist if the prescribed heat fluxes on the channel walls are not uniform. Then, the momentum and energy balance equations are solved by a perturbation method such that the forced convection flow is considered as the base heat transfer process and the effect of buoyancy is evaluated by means of power series expansions with respect to the ratio between the Grashof number and the Reynolds number.

2. Problem statement and theoretical approach

The problem under consideration is that of laminar and fully developed flow between two vertical parallel planes. The distance between the planes is $2L$. The

problem is two-dimensional and a Cartesian coordinate system is chosen such that the transverse coordinate is Y and the coordinate in the direction parallel to the planes is X . The origin of the axes is such that the channel walls are at positions $Y = -L$ and $Y = L$. The X -axis has a direction opposite to the gravitational acceleration. The Boussinesq approximation is assumed to hold and, for the evaluation of the gravitational body force, the mass density is assumed to depend on temperature according to the equation of state

$$\rho = \rho_0[1 - \beta(T - T_0)]. \quad (1)$$

In Eq. (1), the reference temperature is chosen as the mean temperature in a channel section, i.e.

$$T_0 = \frac{1}{2L} \int_{-L}^L T dY. \quad (2)$$

At each channel section, this choice ensures that the averaged square deviation from the local temperature is minimum. As a consequence, Eq. (2) yields the best conditions for the validity of Eq. (1). However, it should be pointed out that T_0 evaluated through Eq. (2) is, in general, a function of X . Then, also ρ_0 should be considered as a function of X and not as a constant. In the following, the approximation stated by Morton [14] in a study on mixed convection in vertical circular ducts will be adopted. Morton's approximation is as follows. If the reference temperature depends on the streamwise coordinate, the value of the reference mass density ρ_0 as well as those of the other thermophysical properties β , k , c_p and μ should be referred to a fixed value of the reference temperature T_0 as, for instance, that at $X=0$. Hence, the properties ρ_0 , β , k , c_p and μ are treated as constants.

The condition of fully developed flow implies that $\partial U/\partial X=0$. Then, since the velocity field \mathbf{U} is solenoidal, one obtains $\partial V/\partial Y=0$. As a consequence, the component V is constant in any channel section and is equal to zero at the channel walls, so that V must be vanishing at any position. The Y -momentum balance equation can be expressed as $\partial P/\partial Y=0$. Therefore, P depends only on X and the X -momentum balance equation is given by

$$\beta g(T - T_0) - \frac{1}{\rho_0} \frac{dP}{dX} + \nu \frac{d^2 U}{dY^2} = 0. \quad (3)$$

If both sides of Eq. (3) are derived with respect to Y , one obtains

$$\frac{\partial T}{\partial Y} = -\frac{\nu}{\beta g} \frac{d^3 U}{dY^3}. \quad (4)$$

Eq. (4) implies that $\partial T/\partial Y$ must be independent of X .

This condition must hold also at the channel walls, where the prescribed heat fluxes are expressed as $-k\partial T/\partial Y$. As a consequence, one is led to the following outcome:

- prescribed wall heat flux distributions which depend on the streamwise coordinate X are not compatible with the condition of fully developed flow.

It should be pointed out that this conclusion is not based on the choice of the reference temperature given by Eq. (2). Indeed, the same conclusion is reached for every choice of a reference temperature which depends at most on X . In the following, it will be assumed that the prescribed wall heat fluxes are uniform. On account of the properties of second order derivatives, if $\partial T/\partial Y$ is independent of X , then $\partial T/\partial X$ must be independent of Y . Then, on account of Eq. (2), one obtains

$$\frac{\partial T}{\partial X} = \frac{dT_0}{dX}. \quad (5)$$

By employing Eq. (5), it is easily verified that the dimensionless temperature $\theta = k(T - T_0)/(\mu U_0^2)$ does not depend on the streamwise coordinate X .

By deriving both sides of Eq. (3) with respect to X , one obtains

$$\frac{\partial T}{\partial X} = \frac{dT_0}{dX} + \frac{1}{\rho_0 \beta g} \frac{d^2 P}{dX^2}. \quad (6)$$

A comparison between Eqs. (5) and (6), leads to the conclusion that dP/dX is a constant.

On account of Eq. (5), the energy balance equation can be written as

$$k \frac{\partial^2 T}{\partial Y^2} + \mu \left(\frac{dU}{dY} \right)^2 = \rho_0 c_p U \frac{dT_0}{dX} - k \frac{d^2 T_0}{dX^2}. \quad (7)$$

Since $\partial T/\partial Y$ is independent of X , if both sides of Eq. (7) are derived with respect to X , one obtains

$$\rho_0 c_p U \frac{d^2 T_0}{dX^2} - k \frac{d^3 T_0}{dX^3} = 0. \quad (8)$$

A further derivation of both sides of Eq. (8) with respect to Y , yields

$$\rho_0 c_p \frac{dU}{dY} \frac{d^2 T_0}{dX^2} = 0. \quad (9)$$

Eq. (9) could be satisfied if dU/dY were zero in the whole interval $-L \leq Y \leq L$. However, on account of the no slip boundary conditions on the fluid velocity, it is easily verified that this condition cannot hold unless the fluid is at rest. As a consequence, Eq. (9) can be fulfilled only if dT_0/dX is a constant. Then, on

account of Eq. (5), one is led to the following conclusion:

- prescribed wall temperature distributions which depend on the streamwise coordinate X and have non-vanishing second order derivatives with respect to X are not compatible with the condition of fully developed flow.

Since dT_0/dX is a constant, the energy balance expressed by Eq. (7) is simplified and assumes the form

$$k \frac{\partial^2 T}{\partial Y^2} + \mu \left(\frac{dU}{dY} \right)^2 = \rho_0 c_p U \frac{dT_0}{dX}. \quad (10)$$

The mean velocity in a channel section is defined as

$$U_0 = \frac{1}{2L} \int_{-L}^L U dY. \quad (11)$$

An integration of both sides of Eq. (10) with respect to Y in the interval $[-L, L]$ yields

$$\begin{aligned} k \frac{\partial T}{\partial Y} \Big|_{Y=L} - k \frac{\partial T}{\partial Y} \Big|_{Y=-L} + \mu \int_{-L}^L \left(\frac{dU}{dY} \right)^2 dY \\ = 2L \rho_0 c_p U_0 \frac{dT_0}{dX}. \end{aligned} \quad (12)$$

The boundary conditions on the temperature field are given by

$$-k \frac{\partial T}{\partial Y} \Big|_{Y=-L} = q_-, \quad k \frac{\partial T}{\partial Y} \Big|_{Y=L} = q_+, \quad (13)$$

so that Eq. (12) can be rewritten as

$$q_- + q_+ + \mu \int_{-L}^L \left(\frac{dU}{dY} \right)^2 dY = 2L \rho_0 c_p U_0 \frac{dT_0}{dX}. \quad (14)$$

By defining the dimensionless parameter

$$\eta = \frac{4L}{\mu U_0^2} \left[q_- + q_+ + \mu \int_{-L}^L \left(\frac{dU}{dY} \right)^2 dY \right], \quad (15)$$

Eq. (14) can be rewritten as

$$\frac{dT_0}{dX} = \frac{\nu U_0}{8L^2 c_p} \eta. \quad (16)$$

On account of Eqs. (15) and (16), the special case $\eta = 0$ implies that $dT_0/dX = 0$ and, as a consequence of Eq. (5), implies also that $\partial T/\partial X = 0$. Then, if $\eta = 0$, one recovers a condition of uniform wall temperatures. If viscous dissipation is negligible, this condition is achieved for $q_- = -q_+$. Otherwise, the sum $q_- + q_+$

must balance the power per unit boundary area generated by viscous dissipation within the channel.

Substitution of Eq. (16) in Eq. (10) yields

$$k \frac{\partial^2 T}{\partial Y^2} + \mu \left(\frac{dU}{dY} \right)^2 = \frac{\mu U_0}{8L^2} \eta U. \tag{17}$$

Eqs. (3) and (17) can be expressed in terms of dimensionless quantities as follows:

$$\frac{d^2 u}{dy^2} = -\frac{Gr}{16Re} \theta - \lambda, \tag{18}$$

$$\frac{d^2 \theta}{dy^2} = -\left(\frac{du}{dy} \right)^2 + \frac{\eta}{8} u. \tag{19}$$

Moreover, the no slip boundary conditions and the thermal boundary conditions given by Eq. (13) can be expressed as

$$u(-1) = u(1) = 0, \tag{20}$$

$$\left. \frac{d\theta}{dy} \right|_{y=-1} = -\frac{1}{4Br}, \quad \left. \frac{d\theta}{dy} \right|_{y=1} = \frac{R}{4Br}. \tag{21}$$

Additional constraints on the dimensionless functions $u(y)$ and $\theta(y)$ are induced by Eqs. (2) and (11), i.e.

$$\int_{-1}^1 u(y) dy = 2, \quad \int_{-1}^1 \theta(y) dy = 0. \tag{22}$$

For any given value of R , Br and Gr/Re , Eqs. (18)–(22) yield the dimensionless velocity profile, the dimensionless temperature profile and the values of the parameters λ and η .

The special case of adiabatic walls is obtained by taking the limits $Br \rightarrow \infty$ and $Br/R \rightarrow \infty$ in Eq. (21).

The Fanning friction factors can be expressed as

$$f_- Re = \left. \frac{8L}{U_0} \frac{dU}{dY} \right|_{Y=-L} = 8 \left. \frac{du}{dy} \right|_{y=-1},$$

$$f_+ Re = -\left. \frac{8L}{U_0} \frac{dU}{dY} \right|_{Y=L} = -8 \left. \frac{du}{dy} \right|_{y=1}. \tag{23}$$

On account of Eqs. (22) and (23), by integrating both sides of Eq. (18) with respect to y in the interval $[-1, 1]$, one obtains

$$f_- + f_+ = \frac{16\lambda}{Re}. \tag{24}$$

Eq. (24) expresses the relation between the Fanning friction factors f_- , f_+ and the pressure drop parameter λ .

The Nusselt numbers are defined by considering as

characteristic temperature difference the difference between the wall temperature and the mean temperature across a channel section, T_0 , namely

$$Nu_- = \frac{4Lq_-}{k[T(-L) - T_0]} = \frac{1}{Br\theta(-1)},$$

$$Nu_+ = \frac{4Lq_+}{k[T(L) - T_0]} = \frac{R}{Br\theta(1)}. \tag{25}$$

Although the bulk temperature is more customary in the definition of the Nusselt number, the mean temperature is sometimes convenient, as in this case. The same choice of the characteristic temperature difference for the definition of the Nusselt number has been made, for instance, by Morton [14].

3. Perturbation series solution

If the dimensionless parameters R and Br are fixed, the functions $u(y)$ and $\theta(y)$ which solve Eqs. (18)–(22) as well as the parameters λ and η can be expressed as power series with respect to the ratio Gr/Re , i.e.

$$u(y) = u_0(y) + u_1(y) \frac{Gr}{Re} + u_2(y) \left(\frac{Gr}{Re} \right)^2 + \dots$$

$$= \sum_{n=0}^{\infty} u_n(y) \left(\frac{Gr}{Re} \right)^n, \tag{26}$$

$$\theta(y) = \theta_0(y) + \theta_1(y) \frac{Gr}{Re} + \theta_2(y) \left(\frac{Gr}{Re} \right)^2 + \dots$$

$$= \sum_{n=0}^{\infty} \theta_n(y) \left(\frac{Gr}{Re} \right)^n, \tag{27}$$

$$\lambda = \lambda_0 + \lambda_1 \frac{Gr}{Re} + \lambda_2 \left(\frac{Gr}{Re} \right)^2 + \dots = \sum_{n=0}^{\infty} \lambda_n \left(\frac{Gr}{Re} \right)^n, \tag{28}$$

$$\eta = \eta_0 + \eta_1 \frac{Gr}{Re} + \eta_2 \left(\frac{Gr}{Re} \right)^2 + \dots = \sum_{n=0}^{\infty} \eta_n \left(\frac{Gr}{Re} \right)^n. \tag{29}$$

An exhaustive description of perturbation methods in heat transfer can be found in ref. [15]. A brief outline of the perturbation method can be given as follows. One substitutes Eqs. (26)–(29) into Eqs. (18)–(22) and collects terms having like powers of the ratio Gr/Re . Then, one equates to zero the coefficient of each power of Gr/Re , thus obtaining a sequence of boundary value problems. The iterative solution of these differential problems allows one to evaluate the functions $u_n(y)$, $\theta_n(y)$ and the dimen-

sionless coefficients λ_n and η_n . The boundary value problem of order $n=0$ is the following:

$$\frac{d^2 u_0}{dy^2} = -\lambda_0, \quad u_0(-1) = u_0(1) = 0, \tag{31}$$

$$\int_{-1}^1 u_0(y) dy = 2,$$

$$\frac{d^2 \theta_0}{dy^2} = -\left(\frac{du_0}{dy}\right)^2 + \frac{\eta_0}{8} u_0,$$

$$\frac{d\theta_0}{dy} \Big|_{y=-1} = -\frac{1}{4Br}, \quad \frac{d\theta_0}{dy} \Big|_{y=1} = \frac{R}{4Br}, \tag{32}$$

$$\int_{-1}^1 \theta_0(y) dy = 0.$$

The solution of Eq. (31) allows one to determine $u_0(y)$ and λ_0 , namely

$$u_0(y) = \frac{3}{2}(1 - y^2), \quad \lambda_0 = 3. \tag{33}$$

On account of Eq. (33), also Eq. (32) can be easily solved and yields

$$\theta_0(y) = -\frac{1}{64Br} \left[(72Br + R + 1)y^4 - 6(24Br + R + 1)y^2 - 8(R - 1)y + \frac{3}{5}(3 + 56Br + 3R) \right],$$

$$\eta_0 = 24 + \frac{R + 1}{Br}. \tag{34}$$

Obviously, Eqs. (33) and (34) describe the fluid flow and heat transfer behavior in the special case of forced convection, i.e. in the limit $Gr \rightarrow 0$. In particular, Eq. (33) yields the usual Hagen–Poiseuille velocity profile, and, by employing Eq. (23), one is led to the usual result

$$f_- Re = 24 = f_+ Re. \tag{35}$$

Eqs. (25) and (34) yield the Nusselt numbers in the case of forced convection, i.e.

$$Nu_- = \frac{40}{24Br - 3R + 7}, \quad Nu_+ = \frac{40R}{24Br + 7R - 3}. \tag{36}$$

Eq. (36) allows one to conclude that Nu_- is singular for $Br = (3R - 7)/24$ and is positive for $Br > (3R - 7)/24$. On the other hand, Nu_+ is singular for $Br = (3 - 7R)/24$ and is positive for $Br/R > (3 - 7R)/(24R)$. Obviously, the singularity of Nu_- corresponds to a value of Br

which yields $T(-L) = T_0$, while the singularity of Nu_+ occurs for a value of Br such that $T(L) = T_0$.

The boundary value problem which corresponds to an arbitrary $n > 0$ can be expressed as

$$\frac{d^2 u_n}{dy^2} = -\frac{\theta_{n-1}}{16} - \lambda_n,$$

$$u_n(-1) = u_n(1) = 0, \quad \int_{-1}^1 u_n(y) dy = 0, \tag{37}$$

$$\frac{d^2 \theta_n}{dy^2} = -\sum_{j=0}^n \left(\frac{du_j}{dy} \frac{du_{n-j}}{dy} - \frac{\eta_j}{8} u_{n-j} \right),$$

$$\frac{d\theta_n}{dy} \Big|_{y=-1} = 0 = \frac{d\theta_n}{dy} \Big|_{y=1}, \quad \int_{-1}^1 \theta_n(y) dy = 0. \tag{38}$$

By solving Eq. (37), one obtains expressions of $u_n(y)$ and λ_n , namely

$$u_n(y) = \frac{\lambda_n}{2}(1 - y^2) + \frac{1 + y}{32} \int_{-1}^1 dy'' \int_0^{y''} dy' \theta_{n-1}(y')$$

$$- \frac{1}{16} \int_{-1}^y dy'' \int_0^{y''} dy' \theta_{n-1}(y'),$$

$$\lambda_n = \frac{3}{32} \left[\int_{-1}^1 dy \int_{-1}^y dy'' \int_0^{y''} dy' \theta_{n-1}(y') - \int_{-1}^1 dy'' \int_0^{y''} dy' \theta_{n-1}(y') \right]. \tag{39}$$

If $\theta_{n-1}(y)$ is known, Eq. (39) yields $u_n(y)$ and λ_n . On account of Eq. (38), one is led to the following expressions of $\theta_n(y)$ and η_n :

$$\theta_n(y) = \frac{1}{2} \sum_{j=0}^n \int_{-1}^1 dy \int_0^y dy'' \int_{-1}^{y''} dy' \times \left[\frac{du_j(y')}{dy'} \frac{du_{n-j}(y')}{dy'} - \frac{\eta_j}{8} u_{n-j}(y') \right]$$

$$- \sum_{j=0}^n \int_0^y dy'' \int_{-1}^{y''} dy' \times \left[\frac{du_j(y')}{dy'} \frac{du_{n-j}(y')}{dy'} - \frac{\eta_j}{8} u_{n-j}(y') \right],$$

$$\eta_n = 4 \sum_{j=0}^n \int_{-1}^1 \frac{du_j(y')}{dy'} \frac{du_{n-j}(y')}{dy'} dy'. \tag{40}$$

If the functions $u_j(y)$ are known for every j such that $0 \leq j \leq n$ and the parameters η_j are known for every j such that $0 \leq j \leq n-1$, Eq. (40) allows one to obtain $\theta_n(y)$ and η_n .

In particular, by the perturbation method described above, one can easily evaluate the lowest order corrections to the forced convection values of the parameters λ , η , f_- , f_+ , Nu_- and Nu_+ , namely

$$\lambda \cong 3 + \frac{3(16Br + R + 1)}{4480Br} \frac{Gr}{Re}, \tag{41}$$

$$\eta \cong 24 + \frac{R + 1}{Br} + \frac{11,232Br^2 + 1236Br(R + 1) + 708R^2 - 1279R + 708}{62,092,800Br^2} \left(\frac{Gr}{Re}\right)^2, \tag{42}$$

$$f_- Re \cong 24 + \frac{72Br - 13R + 22}{840Br} \frac{Gr}{Re}, \tag{43}$$

$$f_+ Re \cong 24 + \frac{72Br + 22R - 13}{840Br} \frac{Gr}{Re}, \tag{44}$$

$$\frac{1}{Nu_-} \cong \frac{24Br - 3R + 7}{40} + \frac{8640Br^2 - 48Br(149R - 166) + (R + 1)(101R - 109)}{4,838,400Br} \frac{Gr}{Re}, \tag{45}$$

$$\frac{1}{Nu_+} \cong \frac{24Br + 7R - 3}{40R} + \frac{8640Br^2 + 48Br(166R - 149) - (R + 1)(109R - 101)}{4,838,400RBr} \frac{Gr}{Re}. \tag{46}$$

4. Symmetric wall heat fluxes

In this section, a special case is examined, i.e. the case $q_- = q_+$, which implies $R = 1$. This value of R leads to temperature and velocity profiles which are symmetric with respect to the plane $Y = 0$. As a consequence, $Nu_- = Nu_+$ and, on account of Eq. (24), $f_- Re = f_+ Re = 8\lambda$.

The evaluations of $u(y)$, $\theta(y)$, λ and η have been performed by employing perturbation series truncated to the first 41 terms. When a perturbation method is employed, it is quite important to know if the perturbation series have a finite radius of convergence r_c . It is easily checked that, for a fixed value of Br , all the perturbation series expressed by Eqs. (26)–(29) have the same radius of convergence and that this radius of convergence is finite. Several methods can be employed to evaluate the real positive number r_c such that the perturbation series given by Eqs. (26)–(29) are convergent for $|Gr/Re| < r_c$. The most commonly adopted method is based on the estimation of D’Alembert’s ratio limit by means of Domb–Sykes plots [15]. In the present paper, a different method is employed. In the following, in order to illustrate this method, reference will be made to the perturbation series expressed by

Eq. (28). First, one recognizes that, for sufficiently high values of n , say in the interval $20 \leq n \leq 40$, the coefficients $\log_{10}|\lambda_n|$ represent approximately a linearly decreasing function of n . Then, by a least-squares fit, one evaluates the constant a and the positive constant b such that

$$\log_{10} |\lambda_n| \cong a - bn. \tag{47}$$

Table 1
Symmetric case: radius of convergence r_c of the perturbation series for some values of Br

Br	r_c
$-\infty$	220
-1	230
$-1/6$	270
$-1/10$	390
-10^{-3}	8.20
10^{-3}	6.90
$1/10$	160
$1/6$	200
1	220
$+\infty$	220

It is easily verified that $r_c \cong 10^b$ is an estimate of the radius of convergence. The values of b and, hence, of r_c depend on the choice of Br . In Table 1, values of r_c are reported for various values of Br . This table shows that, for $|Br| \geq 1/10$, the radius of convergence is an increasing function of Br . Although in Table 1 the cases $Br = \infty$ and $Br = -\infty$ are distinguished for convenience, they are mathematically and physically equivalent since they correspond to a channel with adiabatic walls.

The perturbation series solution for small values of Br can be compared with the solution of the boundary value problem in the limit $Br \rightarrow 0$, i.e. in the limit of a negligible viscous dissipation. In order to perform this limit, one can introduce the modified dimensionless quantities

$$\bar{\theta} = Br\theta = k \frac{T - T_0}{4Lq_-}, \quad \overline{Gr} = \frac{Gr}{Br} = \frac{256L^4 g \beta q_-}{kv^2},$$

$$\bar{\eta} = Br\eta = 2 + 4Br \int_{-1}^1 \left(\frac{du}{dy} \right)^2 dy. \tag{48}$$

On account of Eq. (48), Eqs. (18)–(22) for $R=1$ can

while Eq. (55) yields

$$\bar{\theta} = \frac{\cosh \chi \sin \chi + \cos \chi \sinh \chi - \chi [\cosh \chi \cos(\chi y) + \cos \chi \cosh(\chi y)]}{4\chi^2 [\sin \chi \cosh \chi - \cos \chi \sinh \chi]},$$

be rewritten as

$$\frac{d^2 u}{dy^2} = -\frac{\overline{Gr}}{16Re} \bar{\theta} - \lambda, \tag{49}$$

$$\frac{d^2 \bar{\theta}}{dy^2} = -Br \left(\frac{du}{dy} \right)^2 + \frac{\bar{\eta}}{8} u, \tag{50}$$

$$u(-1) = u(1) = 0, \quad \left. \frac{d\bar{\theta}}{dy} \right|_{y=-1} = -\frac{1}{4}, \quad \left. \frac{d\bar{\theta}}{dy} \right|_{y=1} = \frac{1}{4}, \tag{51}$$

$$\int_{-1}^1 u(y) dy = 2, \quad \int_{-1}^1 \bar{\theta}(y) dy = 0. \tag{52}$$

It is easily verified that, in the limit $Br \rightarrow 0$, $\bar{\eta} = 2$ and Eqs. (49)–(52) yield

$$\frac{d^4 u}{dy^4} = -\frac{\overline{Gr}}{64Re} u, \tag{53}$$

$$u(-1) = u(1) = 0, \quad \left. \frac{d^3 u}{dy^3} \right|_{y=-1} = \frac{\overline{Gr}}{64Re}, \tag{54}$$

$$\left. \frac{d^3 u}{dy^3} \right|_{y=1} = -\frac{\overline{Gr}}{64Re},$$

$$\bar{\theta} = -\frac{16Re}{\overline{Gr}} \left(\frac{d^2 u}{dy^2} + \lambda \right),$$

$$\lambda = \frac{1}{2} \left(\left. \frac{du}{dy} \right|_{y=-1} - \left. \frac{du}{dy} \right|_{y=1} \right). \tag{55}$$

Let us define a parameter χ such that

$$\chi^4 = -\frac{\overline{Gr}}{64Re}. \tag{56}$$

As is well known [9], the solution of Eqs. (53) and (54) can be expressed as

$$u(y) = \frac{\chi [\cosh \chi \cos(\chi y) - \cos \chi \cosh(\chi y)]}{\sin \chi \cosh \chi - \cos \chi \sinh \chi}, \tag{57}$$

$$\lambda = \frac{\chi^2 [\cosh \chi \sin \chi + \cos \chi \sinh \chi]}{\sin \chi \cosh \chi - \cos \chi \sinh \chi}. \tag{58}$$

Eqs. (57) and (58) can be employed both in the case $\overline{Gr}/Re < 0$ (buoyancy-opposed flow) and in the case $\overline{Gr}/Re > 0$ (buoyancy-assisted flow). In the former case, χ is a real parameter, while, in the latter case, χ is a complex parameter. As is shown by Eqs. (56)–(58), the solution of Eqs. (49)–(52) in the limit $Br \rightarrow 0$ is uniquely determined by the value of \overline{Gr}/Re . Therefore, on account of Eq. (48), one expects that the solution for a small value of Br , say 10^{-3} , and a given ratio Gr/Re is similar to the solution which corresponds to $Br = -10^{-3}$ and $-Gr/Re$. In any case, both solutions should not be much different from that expressed by Eqs. (57) and (58). This inference can be the basis for a comparison between the perturbation method described in the preceding section and the solution for the case $Br \rightarrow 0$ expressed through Eqs. (57) and (58). Indeed, in Table 2, the values of Nu_+ and λ obtained for $Br = 10^{-3}$ and for $Br = -10^{-3}$ by employing the perturbation method are compared with the values of

Table 2

Symmetric case: values of Nu_+ and λ for $Br = \pm 10^{-3}$, evaluated by the perturbation method, and for $Br = 0$, evaluated by Eqs. (25), (48), (57) and (58)

\overline{Gr}/Re	$Br = 10^{-3}$ perturbation method		$Br = -10^{-3}$ perturbation method		$Br = 0$ closed- form solution	
	Nu_+	λ	Nu_+	λ	Nu_+	λ
-5500	7.376	-8.470	8.125	-7.042	7.805	-7.621
-5000	7.762	-6.727	8.274	-5.890	8.042	-6.256
-4500	8.084	-5.271	8.435	-4.778	8.271	-5.005
-4000	8.365	-4.004	8.606	-3.713	8.490	-3.851
-3500	8.617	-2.872	8.784	-2.699	8.702	-2.783
-3000	8.847	-1.843	8.966	-1.739	8.907	-1.790
-2500	9.058	-0.8964	9.151	-0.8316	9.104	-0.8638
-2000	9.255	-0.01743	9.336	0.02492	9.295	0.003791
-1500	9.441	0.8045	9.520	0.8332	9.480	0.8188
-1000	9.616	1.577	9.703	1.596	9.659	1.587
-500	9.782	2.308	9.883	2.317	9.832	2.313
0	9.940	3.000	10.06	3.000	10.00	3.000
500	10.09	3.659	10.23	3.647	10.16	3.653
1000	10.24	4.287	10.41	4.262	10.32	4.274
1500	10.38	4.888	10.57	4.846	10.47	4.867
2000	10.51	5.464	10.74	5.403	10.62	5.434
2500	10.64	6.017	10.90	5.936	10.77	5.976
3000	10.77	6.549	11.05	6.445	10.91	6.497
3500	10.89	7.062	11.20	6.933	11.05	6.997
4000	11.01	7.556	11.35	7.401	11.18	7.478
4500	11.12	8.034	11.50	7.852	11.31	7.942
5000	11.24	8.496	11.64	8.285	11.44	8.389
5500	11.34	8.944	11.78	8.704	11.56	8.822

these quantities obtained for $Br = 0$ by means of Eqs. (25), (48) and (58). As it should be expected, each value of λ or Nu_+ for $Br = 0$ lies in the interval between the corresponding values for $Br = 10^{-3}$ and for $Br = -10^{-3}$. Moreover, both for λ and for Nu_+ , the differences between the cases $Br = 0$, $Br = 10^{-3}$ and $Br = -10^{-3}$ become more relevant as $|\overline{Gr}/Re|$ increases.

It is easily verified that, in the case $Br = 0$, the closed-form solution expressed by Eqs. (57) and (58) presents singularities for the positive real values of χ which solve the equation

$$\sin \chi \cosh \chi - \cos \chi \sinh \chi = 0. \tag{59}$$

Since reference is made to the positive real roots of Eq. (59), the case $\overline{Gr}/Re < 0$, i.e. buoyancy-opposed flow, is considered. On account of Eqs. (56) and (59), an infinite sequence of values of \overline{Gr}/Re which correspond to singularities of both $u(y)$, $\theta(y)$ and λ exists, namely $\overline{Gr}/Re = -15,214.1, -159,775, -695,525, \dots$. The occurrence of this sequence of singularities means that for $\overline{Gr}/Re = -15,214.1, -159,775, -695,525, \dots$ no solutions of Eqs. (53)–(55) exist. An almost identi-

cal circumstance has been analyzed by Morton [14] with reference to the velocity and temperature profiles in the case of a vertical circular cylinder with a prescribed uniform wall heat flux. In that case, the singularities were evaluated by means of the positive real zeros of the Bessel function of the first kind and order zero. By applying Morton’s viewpoint to the velocity and temperature profiles expressed by Eqs. (57) and (58), one can state that, if $\overline{Gr}/Re < -15,214.1$, ‘there are theoretically possible flows ... which are rather unlikely to be found in practice’. Indeed, for the buoyancy-opposed regime, conceivable laminar flows are those such that $-15,214.1 < \overline{Gr}/Re < 0$. However, it should be emphasized that stability analyses may yield further restrictions of this domain [9].

From a different perspective, it can be pointed out that the velocity and temperature profiles defined by Eqs. (57) and (58) are analytic functions of the variable \overline{Gr}/Re in the open interval $|\overline{Gr}/Re| < 15,214.1$. Thus, these functions can be expressed as power series with respect to \overline{Gr}/Re and these series are convergent for $|\overline{Gr}/Re| < 15,214.1$. On the other hand, Table 1 shows that, for $Br = 10^{-3}$ and for $Br = -10^{-3}$, power series expressions of the velocity and temperature profiles with respect \overline{Gr}/Re to would be convergent only for $|\overline{Gr}/Re| < 6900$ and for $|\overline{Gr}/Re| < 8200$, respectively. As a consequence, the domain of convergence of a power series solution is reduced if the viscous dissipation effect is taken into account, even if the Brinkman number is very small. In particular, the more relevant reduction of the convergence domain occurs if the fluid is heated ($Br = 10^{-3}$).

Table 3

Symmetric case: values of Nu_+ and λ for $Br = \pm 1/6$

Gr/Re	$Br = 1/6$		$Br = -1/6$	
	Nu_+	λ	Nu_+	λ
-150	5.988	0.4175	84.27	2.757
-130	5.973	0.7928	93.65	2.775
-110	5.904	1.138	106.5	2.797
-90	5.796	1.468	125.0	2.822
-70	5.659	1.795	154.1	2.852
-50	5.497	2.124	206.5	2.887
-30	5.313	2.462	328.7	2.928
-10	5.109	2.816	939.7	2.974
0	5.000	3.000	∞	3.000
10	4.886	3.191	-893.0	3.028
30	4.644	3.596	-282.0	3.090
50	4.382	4.042	-159.7	3.161
70	4.101	4.541	-107.1	3.243
90	3.799	5.114	-77.86	3.339
110	3.478	5.787	-59.13	3.452
130	3.139	6.595	-46.05	3.587
150	2.791	7.580	-36.33	3.750

In Table 3, values of Nu_+ and λ are reported for $Br = \pm 1/6$ and for some values of Gr/Re . This table shows that, for $Br = \pm 1/6$, λ is an increasing function of Gr/Re . On the other hand, Nu_+ is a decreasing function of Gr/Re when $Br = 1/6$, while it is an increasing function for $Br = -1/6$. In the case $Br = -1/6$, Table 3 yields an infinite value of Nu_+ for $Gr/Re = 0$. This result is easily deduced from Eq. (36), in the case $R = 1$. The singularity of Nu_+ is no more present whenever $Gr/Re \neq 0$. More precisely, for upward flow ($Gr/Re > 0$), Nu_+ is negative since $T(L) > T_0$ while, for downward flow ($Gr/Re < 0$), Nu_+ is positive since $T(L) < T_0$. Table 3 shows that, as Gr/Re is increased, λ increases more in the case of fluid heating ($Br > 0$) than in the case of fluid cooling ($Br < 0$).

Table 4 refers to the cases $Br = \pm 1$ as well as to the case of adiabatic channel walls, i.e. $Br = \pm \infty$. Obviously, the values of Nu_+ are not reported for $Br = \pm \infty$, since in this case they are zero for every value of Gr/Re . The values of λ for $Br = \pm \infty$ lie within those for $Br = 1$ and those for $Br = -1$. The differences between these values are more and more considerable as $|Gr/Re|$ increases. The values of Nu_+ for $Br = -1$ are negative, because q_+ is negative, but the viscous heating is so intense that $T(L) > T_0$.

Fig. 1 corresponds to $\overline{Gr}/Re = 1080$ and displays the dimensionless velocity and temperature profiles for some values of Br . In particular, the plots of u and $\bar{\theta}$ for $Br = 0$ have been obtained by employing Eqs. (57)

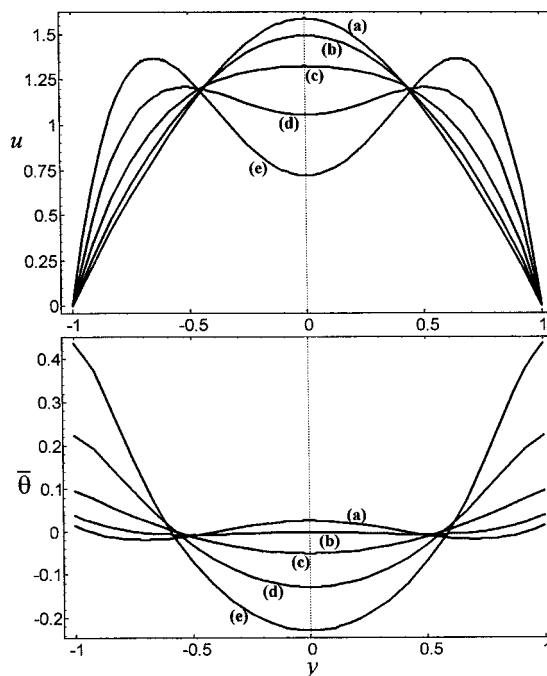


Fig. 1. Symmetric case: plots of u and $\bar{\theta}$ vs y for $\overline{Gr}/Re = 1080$ and for (a) $Br = -1/6$, (b) $Br = -1/10$, (c) $Br = 0$, (d) $Br = 1/10$, (e) $Br = 1/6$.

Table 4

Symmetric case: values of Nu_+ for $Br = \pm 1$ and of λ for $Br = \pm 1$ and for $Br = \pm \infty$

Gr/Re	$Br = 1$		$Br = -1$		$Br = \pm \infty$
	Nu_+	λ	Nu_+	λ	λ
-180	2.069	1.294	-3.233	1.755	1.531
-160	2.007	1.460	-3.086	1.864	1.667
-140	1.942	1.628	-2.942	1.978	1.806
-120	1.874	1.799	-2.801	2.098	1.950
-100	1.804	1.975	-2.663	2.224	2.101
-80	1.733	2.159	-2.526	2.359	2.259
-60	1.659	2.350	-2.392	2.502	2.426
-40	1.584	2.553	-2.261	2.655	2.604
-20	1.507	2.768	-2.130	2.820	2.794
0	1.429	3.000	-2.000	3.000	3.000
20	1.348	3.252	-1.871	3.197	3.224
40	1.265	3.529	-1.743	3.414	3.472
60	1.180	3.838	-1.614	3.658	3.748
80	1.092	4.189	-1.485	3.934	4.062
100	1.001	4.597	-1.354	4.255	4.426
120	0.9054	5.082	-1.220	4.635	4.859
140	0.8060	5.677	-1.083	5.101	5.390
160	0.7027	6.435	-0.9416	5.694	6.067
180	0.5977	7.428	-0.7957	6.486	6.965

and (58). Since Fig. 1 refers to a positive value of \overline{Gr}/Re , the plots for $Br = 1/10$ and $Br = 1/6$ correspond to fluid heating and upward flow, while the plots for $Br = -1/10$ and $Br = -1/6$ correspond to fluid cooling and downward flow. Indeed, Fig. 1 shows that, for positive values of Br , the effect of an increasing viscous dissipation is an increase of the dimensionless fluid velocity next to the channel walls. On the contrary, for negative values of Br , this figure shows that an increase of the viscous heating yields a decrease of the dimensionless fluid velocity next to the channel walls. Fig. 1 reveals that the dimensionless temperature at $y = \pm 1$ is an increasing function of Br . Moreover, the temperature profiles for $Br > 0$ are less uniform than in the case $Br = 0$. For $Br = -1/10$ and $Br = -1/6$, the sign of $d^2\bar{\theta}/dy^2$ at $y = 0$ becomes negative. Since the symmetry implies that du/dy is zero at $y = 0$, Eq. (50) allows one to conclude that a negative value of $d^2\bar{\theta}/dy^2$ at $y = 0$ corresponds to $\bar{\eta}u(0) < 0$. Fig. 1 ensures that $u(0)$ is positive for every Br , so that $\bar{\eta}$ must be negative. Indeed, on account of Eqs. (15) and (48), the condition $\bar{\eta} < 0$ is accomplished for negative Br , provided that the power generated by viscous dissipation within the channel exceeds the power subtracted at the channel walls.

Fig. 2 refers to $\overline{Gr}/Re = -1080$ and displays the distributions of u and $\bar{\theta}$ for some values of Br . In this

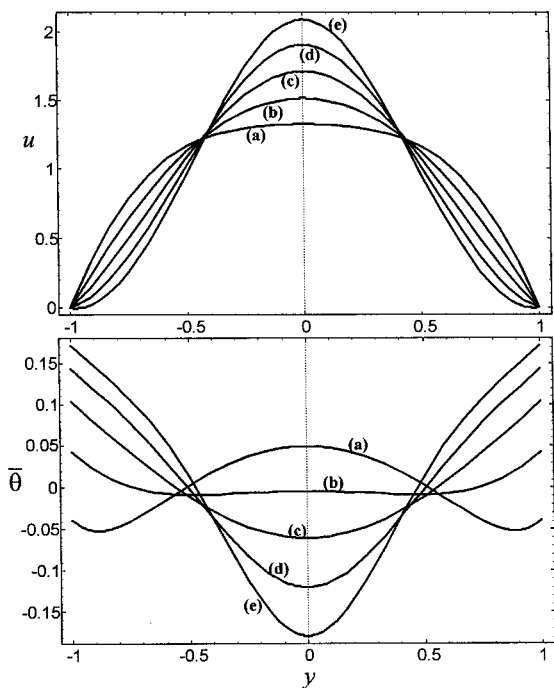


Fig. 2. Symmetric case: plots of u and $\bar{\theta}$ vs y for and for $\overline{Gr}/Re = -1080$ and for (a) $Br = -1/6$, (b) $Br = -1/10$, (c) $Br = 0$, (d) $Br = 1/10$, (e) $Br = 1/6$.

figure, the plots for $Br = 1/10$ and $Br = 1/6$ correspond to fluid heating and downward flow, while the plots for $Br = -1/10$ and $Br = -1/6$ correspond to fluid cooling and upward flow. Fig. 2 shows that, for positive values of Br , an increasing viscous dissipation yields a decrease of the dimensionless fluid velocity next to the channel walls. The reverse occurs for negative values of Br . The same figure shows that the dimensionless temperature at $y = \pm 1$ is an increasing function of Br . Moreover, this figure reveals that, for negative values of Br , the derivative $d^2\bar{\theta}/dy^2$ is negative at $y=0$. The sign of this derivative has the meaning explained in the case of Fig. 1.

Fig. 3 refers to a channel with adiabatic walls. In this case, $Br = \pm \infty$ and the heat transfer within the fluid is due only to viscous heating. The plots of u and θ reported in this figure correspond to different values of the ratio Gr/Re . More precisely, for positive values of Gr/Re , upward flow occurs and both u and θ in the neighborhood of the channel walls are increased with respect to the case of forced convection. On the contrary, for negative values of Gr/Re , downward flow occurs and, in the neighborhood of the channel walls, a decrease of both u and θ with respect to the case of forced convection is observed.

5. Asymmetric wall heat fluxes

In order to inspect the behavior of the velocity and temperature profiles for asymmetric wall heat fluxes ($R \neq 1$), reference is made to $Br = 1/2$ and two test cases are considered: $R = 1/2$ and $R = -1/2$. The former case corresponds to fluid heating at both walls, while the latter case corresponds to fluid heating at the wall $Y = -L$ and fluid cooling at the wall $Y = L$. The evaluations are made by employing the perturbation series expressed by Eqs. (26)–(29) truncated to the first 31 terms. By applying the method described in the preceding section, the radius of convergence is estimated. One obtains $r_c \cong 60$ for $R = 1/2$ and $r_c \cong 55$ for $R = -1/2$.

Figs. 4 and 5 refer to $R = 1/2$ and $R = -1/2$, respectively. Both these figures reveal that the asymmetry of the velocity profiles is more evident for positive values of Gr/Re (upward flow) than for negative values of this parameter (downward flow). Moreover, an analysis of the velocity and temperature profiles allows one to conclude that the effect of buoyancy is more considerable for upward flow than for downward flow. In the case of upward flow, the dimensionless velocity gradient du/dy increases with buoyancy in the neighborhood of $y = -1$ and slightly decreases next to the other wall. As a consequence, both the viscous heating and the fluid temperature are increased by buoyancy in

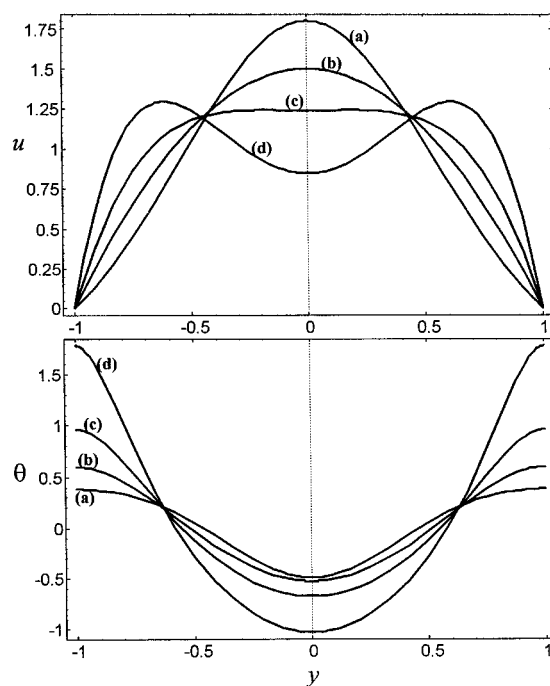


Fig. 3. Symmetric case: plots of u and θ vs y for $Br = \pm \infty$ and for (a) $Gr/Re = -200$, (b) $Gr/Re = 0$, (c) $Gr/Re = 120$, (d) $Gr/Re = 200$.

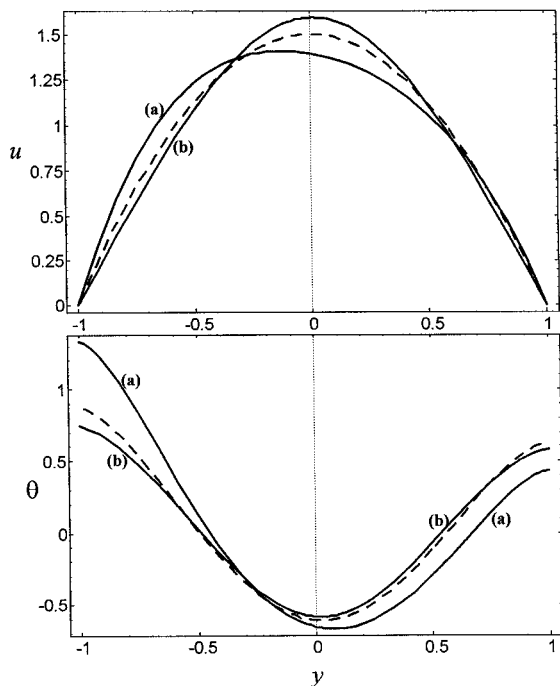


Fig. 4. Asymmetric case: plots of u and θ vs y for $Br=1/2$ and $R=1/2$. The dashed lines refer to $Gr/Re=0$, while the solid lines refer to (a) $Gr/Re=50$ and to (b) $Gr/Re=-50$, respectively.

the region next to $y=-1$, while the opposite occurs next to $y=1$. The main difference between the behaviors for $R=1/2$ and $R=-1/2$ is that, in the first case, the temperature values at $Y=L$ are greater than T_0 , while, in the second case, the temperature values at the cooled wall for $Gr/Re=50$ are smaller than T_0 . Indeed, Fig. 5 shows that for $R=-1/2$ there exists a positive value of Gr/Re such that $T(L)=T_0$, i.e. a value of Gr/Re which corresponds to a singularity of Nu_+ . This value is approximately equal to 35.5.

6. Conclusions

Laminar mixed convection in a vertical parallel-plate channel with prescribed wall heat fluxes has been analyzed in the fully developed regime by taking into account the effect of viscous dissipation. The Boussinesq approximation has been adopted by employing the mean temperature in a channel section as the reference temperature. Morton's approximation has been used to neglect the streamwise changes of the fluid properties. According to this mathematical model, it has been shown that:

1. the condition of fully developed flow is not compat-

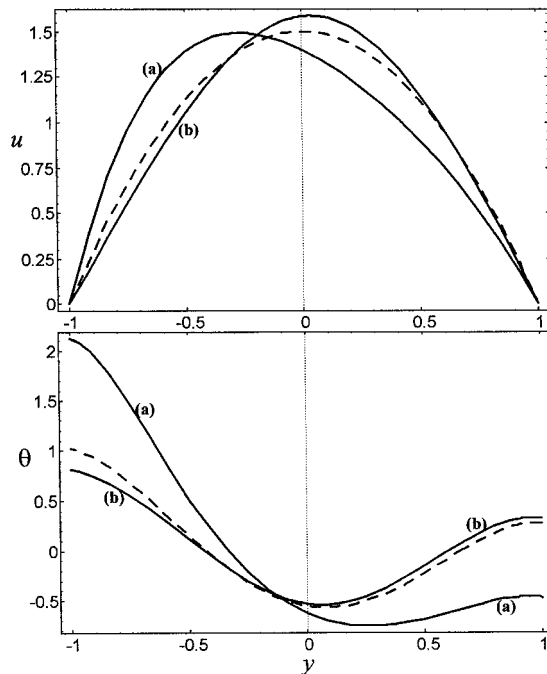


Fig. 5. Asymmetric case: plots of u and θ vs y for $Br=1/2$ and $R=-1/2$. The dashed lines refer to $Gr/Re=0$, while the solid lines refer to (a) $Gr/Re=50$ and to (b) $Gr/Re=-50$, respectively.

ible with changes of the wall heat flux distributions in the streamwise direction;

2. the condition of fully developed flow is not compatible with wall temperature distributions which cannot be expressed as linear functions of the streamwise coordinate.

The momentum balance and the energy balance equations have been solved by employing a perturbation method based on power series expansions with respect to the ratio between the Grashof number and the Reynolds number, Gr/Re . Indeed, according to the perturbation method, the forced convection flow has been considered as the base heat transfer process and corrections of this base process of order $(Gr/Re)^n$ have been evaluated for every positive integer n . The radius of convergence of the perturbation series has been estimated and has been shown to depend on the Brinkman number Br and on the heat fluxes ratio R .

A special attention has been devoted to the case of symmetric wall heat fluxes ($R=1$). In this case, a comparison has been performed between the perturbation solution with small values of Br and the closed-form solution obtained in the case of a negligible viscous dissipation. It has been pointed out that, even for $|Br|=10^{-3}$, the effect of viscous dissipation is not negligible especially for high values of Gr/Re . The Nusselt

number and the pressure drop parameter have been evaluated as functions of Gr/Re for some values of Br . The effect of viscous dissipation on the behavior of the velocity and temperature profiles has been illustrated. In the case of an infinite Brinkman number, i.e. in the case of a channel with adiabatic walls, the velocity and temperature profiles have been analyzed for some values of the ratio Gr/Re . It has been shown that the effect of viscous dissipation is almost dominant for $|Br| \gtrsim 1$. Indeed, the values of the pressure drop parameter for $|Br|=1$ are similar to those for $|Br|=\infty$.

The case of asymmetric wall heat fluxes has been investigated for $Br=1/2$ with either $R=1/2$ or $R=-1/2$. It has been pointed out that, for $R=-1/2$, there exists a positive value of Gr/Re which yields a temperature on the cooled wall equal to the mean temperature and, as a consequence, an infinite Nusselt number on the cooled wall.

References

- [1] L.S. Yao, Free and forced convection in the entry region of a heated vertical channel, *International Journal of Heat and Mass Transfer* 26 (1983) 65–72.
- [2] W. Aung, G. Worku, Developing flow and flow reversal in a vertical channel with asymmetric wall temperatures, *ASME Journal of Heat Transfer* 108 (1986) 299–304.
- [3] W. Aung, G. Worku, Theory of fully developed, combined convection including flow reversal, *ASME Journal of Heat Transfer* 108 (1986) 485–488.
- [4] W. Aung, G. Worku, Mixed convection in ducts with asymmetric wall heat fluxes, *ASME Journal of Heat Transfer* 109 (1987) 947–951.
- [5] A.S. Lavine, Analysis of fully developed opposing mixed convection between inclined parallel plates, *Wärme- und Stoffübertragung* 23 (1988) 249–257.
- [6] C-H. Cheng, H-S. Kou, W-H. Huang, Flow reversal and heat transfer of fully developed mixed convection in vertical channels, *Journal of Thermophysics* 4 (1990) 375–383.
- [7] T.T. Hamadah, R.A. Wirtz, Analysis of laminar fully developed mixed convection in a vertical channel with opposing buoyancy, *ASME Journal of Heat Transfer* 113 (1991) 507–510.
- [8] A.S. Lavine, On the linear stability of mixed and free convection between inclined parallel plates with fixed heat flux boundary conditions, *International Journal of Heat and Mass Transfer* 36 (1993) 1373–1387.
- [9] Y-C. Chen, J.N. Chung, The linear stability of mixed convection in a vertical channel flow, *Journal of Fluid Mechanics* 325 (1996) 29–51.
- [10] Y-C. Chen, J.N. Chung, Stability of mixed convection in a differentially heated vertical channel, *ASME Journal of Heat Transfer* 120 (1998) 127–132.
- [11] A. Barletta, Laminar mixed convection with viscous dissipation in a vertical channel, *International Journal of Heat and Mass Transfer* 41 (1998) 3501–3513.
- [12] E. Zanchini, Effect of viscous dissipation on mixed convection in a vertical channel with boundary conditions of the third kind, *International Journal of Heat and Mass Transfer* 41 (1998) 3949–3959.
- [13] R.K. Shah, A.L. London, *Laminar Flow Forced Convection in Ducts*, Academic Press, New York, 1978.
- [14] B.R. Morton, Laminar convection in uniformly heated vertical pipes, *Journal of Fluid Mechanics* 8 (1960) 227–240.
- [15] A. Aziz, T.Y. Na, *Perturbation Methods in Heat Transfer*, Hemisphere, Washington, DC, 1984.